A storage ring experiment to detect a proton electric dipole moment

V. Anastassopoulos,[1] S. Andrianov,[2] R. Baartman,[3] S. Baessler,[4] M. Bai,[5] J. Benante,[6] M. Berz,[7] M. Blaskiewicz,[6] T. Bowcock,[8] K. Brown,[6] B. Casey,[9] M. Conte,[10] J. D. Crnkovic,[6] N. D'Imperio,[6] G. Fanourakis,[11] A. Fedotov,[6] P. Fierlinger,[12] W. Fischer,[6] M. O. Gaisser,[13] Y. Giomataris,[14] M. Grosse-Perdekamp,[15] G. Guidoboni,[16] S. Hacıömeroğlu,[13] G. Hoffstaetter,[17] H. Huang,[6] M. Incagli,[18] A. Ivanov,[2] D. Kawall,[19] Y. I. Kim,[13] B. King,[8] I. A. Koop,[20] D. M. Lazarus,[6] V. Lebedev,[9] M. J. Lee,[13] S. Lee,[13] Y. H. Lee,[21] A. Lehrach,[5,22] P. Lenisa,[16] P. Levi Sandri,[23] A. U. Luccio,[6] A. Lyapin,[24] W. MacKay,[6] R. Maier,[5] K. Makino,[7] N. Malitsky,[6] W. J. Marciano,[6] W. Meng,[6] F. Meot,[6] E. M. Metodiev,[13,25] L. Miceli,[13] D. Moricciani,[26] W. M. Morse,[6] S. Nagaitsev,[9] S. K. Nayak,[6] Y. F. Orlov,[17] C. S. Ozben,[27] S. T. Park,[13] A. Pesce,[16] E. Petrakou,[13] P. Pile,[6] B. Podobedov,[6] V. Polychronakos,[6] J. Pretz,[22] V. Ptitsyn,[6] E. Ramberg,[9] D. Raparia,[6] F. Rathmann,[5] S. Rescia,[6] T. Roser,[6] H. Kamal Sayed,[6] Y. K. Semertzidis,[13,28,a)] Y. Senichev,[5] A. Sidorin,[29] A. Silenko,[29,30] N. Simos,[6] A. Stahl,[22] E. J. Stephenson,[31] H. Ströher,[5] M. J. Syphers,[9,32] J. Talman,[6] R. M. Talman,[17] V. Tishchenko,[6] C. Touramanis,[8] N. Tsoupas,[6] G. Venanzoni,[23] K. Vetter,[33] S. Vlassis,[1] E. Won,[13,34] G. Zavattini,[16] A. Zelenski,[6] and K. Zioutas[1]

[1]*Department of Physics, University of Patras, 26500 Rio-Patras, Greece*
[2]*Faculty of Applied Mathematics and Control Processes, Saint-Petersburg State University, Saint-Petersburg, Russia*
[3]*TRIUMF, 4004 Wesbrook Mall, Vancouver, British Columbia V6T2A3, Canada*
[4]*Department of Physics, University of Virginia, Charlottesville, Virginia 22904, USA*
[5]*Institut für Kernphysik and JARA-Fame, Forschungszentrum Jülich, 52425 Jülich, Germany*
[6]*Brookhaven National Laboratory, Upton, New York 11973, USA*
[7]*Department of Physics and Astronomy, Michigan State University, East Lansing, Michigan 48824, USA*
[8]*Department of Physics, University of Liverpool, Liverpool, United Kingdom*
[9]*Fermi National Accelerator Laboratory, Batavia, Illinois 60510, USA*
[10]*Physics Department and INFN Section of Genoa, 16146 Genoa, Italy*
[11]*Institute of Nuclear and Particle Physics NCSR Demokritos, GR-15310 Aghia Paraskevi Athens, Greece*
[12]*Technical University München, Physikdepartment and Excellence-Cluster "Universe," Garching, Germany*
[13]*Center for Axion and Precision Physics Research, Institute for Basic Science (IBS), Daejeon 34141, South Korea*
[14]*CEA/Saclay, DAPNIA, 91191 Gif-sur-Yvette Cedex, France*
[15]*Department of Physics, University of Illinois at Urbana-Champaign, Urbana, Illinois 61801, USA*
[16]*University of Ferrara, INFN of Ferrara, Ferrara, Italy*
[17]*Laboratory for Elementary-Particle Physics, Cornell University, Ithaca, New York 14853, USA*
[18]*Physics Department, University and INFN Pisa, Pisa, Italy*
[19]*Department of Physics, University of Massachusetts, Amherst, Massachusetts 01003, USA*
[20]*Budker Institute of Nuclear Physics, 630090 Novosibirsk, Russia*
[21]*Korea Research Institute of Standards and Science, Daejeon 34141, South Korea*
[22]*RWTH Aachen University and JARA-Fame, III. Physikalisches Institut B, Physikzentrum, 52056 Aachen, Germany*
[23]*Laboratori Nazionali di Frascati, INFN, I-00044 Frascati, Rome, Italy*
[24]*Royal Holloway, University of London, Egham, Surrey, United Kingdom*
[25]*Harvard College, Harvard University, Cambridge, Massachusetts 02138, USA*
[26]*Dipartimento di Fisica dell'Univ. di Roma "Tor Vergata" and INFN Sezione di Roma Tor Vergata, Rome, Italy*
[27]*Istanbul Technical University, Istanbul 34469, Turkey*
[28]*Department of Physics, Korea Advanced Institute of Science and Technology (KAIST), Daejeon 34141, South Korea*
[29]*Joint Institute for Nuclear Research, Dubna, Moscow region, Russia*
[30]*Research Institute for Nuclear Problems of Belarusian State University, Minsk, Belarus*
[31]*Indiana University Center for Spacetime Symmetries, Bloomington, Indiana 47405, USA*
[32]*Department of Physics, Northern Illinois University, DeKalb, Illinois 60115, USA*
[33]*Oak Ridge National Laboratory, Oak Ridge, Tennessee 37831, USA*
[34]*Physics Department, Korea University, Seoul 02841, South Korea*

(Received 11 June 2016; accepted 27 October 2016; published online 29 November 2016)

A new experiment is described to detect a permanent electric dipole moment of the proton with a sensitivity of 10^{-29} $e \cdot$ cm by using polarized "magic" momentum 0.7 GeV/c protons in an all-electric storage ring. Systematic errors relevant to the experiment are discussed and

a)Author to whom correspondence should be addressed. Electronic mail: yannis@kaist.ac.kr

techniques to address them are presented. The measurement is sensitive to new physics beyond the standard model at the scale of 3000 TeV. [http://dx.doi.org/10.1063/1.4967465]

I. INTRODUCTION

One of the outstanding problems in contemporary elementary particle physics and cosmology is finding an explanation for the observed matter-antimatter asymmetry of our universe, known as baryogenesis. Within the framework of the Big Bang, it appears that a much greater degree of CP-violation than provided by the standard model of particle physics is required. That suggests the necessary existence of New Physics (NP), with large CP-violating interactions as a key ingredient in understanding the early universe. Identifying that NP source, central to our very existence, would be a major intellectual achievement.

In the search for laboratory manifestations of new CP-violating effects, electric dipole moments (EDMs) play a crucial role. A non-zero permanent particle electric dipole moment (EDM) separately violates parity (P) and time reversal symmetry (T).[1] So, assuming CPT invariance (the combined symmetry over C-charge, P-parity and T-time), CP must also be violated. Since standard model EDM predictions are much smaller than current experimental sensitivities, an observation of any particle's EDM with today's technology would signal the discovery of NP. If of sufficient strength, such a source could provide a possible explanation for baryogenesis. Some theories, which suggest that an EDM may be within experimental reach, include supersymmetry (SUSY),[2] left-right symmetry,[3] and multi-Higgs scenarios.[4] Here, we explore the possibility of a storage ring search and study of the proton EDM (d_p) at an unprecedented level of 10^{-29} $e\cdot$cm, an advance by nearly 5 orders of magnitude beyond the current indirect bound of $|d_p| < 7.9\times10^{-25}$ $e\cdot$cm obtained using Hg atoms.[5] Observing the EDM from different simple systems is necessary to identify the source of any NP.[6]

This dedicated direct proton EDM study at the level of 10^{-29} $e\cdot$cm is sensitive to a generic NP mass scale $\Lambda_{\rm NP}$ with CP-violating phase $\phi_{\rm NP}$ roughly satisfying[7] $(3000\ {\rm TeV}/\Lambda_{\rm NP})^2 \tan(\phi_{\rm NP}) > 1$. For a phase of the order of 45 degrees, the 3000 TeV NP scale is being probed, while for NP generically parametrized by a scale of order 1 TeV, a relative phase sensitivity as small as $\phi_{\rm NP}\approx10^{-7}$ would be reached. Many specific examples of the outstanding probing power of a proton EDM study at the 10^{-29} $e\cdot$cm level exist. Here, we point out that it constrains the $\theta_{\rm QCD}$ parameter at 10^{-13}, 3 orders of magnitude below the current neutron EDM bounds. A more timely illustration in the current LHC (the Large Hadron Collider at CERN in Switzerland) era is a potential CP-violating chiral phase induced by a loop induced Higgs to 2-photon coupling (the relative pseudoscalar to scalar amplitudes, a measure of potential Higgs CP-violation). Such an effective coupling would lead to fermion EDMs via quantum loops, making for an overall effect of 2-loop order. The proton EDM experimental program envisioned in this paper would be sensitive to a relative pseudoscalar coupling of order 10^{-3}, about 2 orders of magnitude below current electron EDM constraints. It should be noted that EDMs of the electron, proton, and neutron may actually represent our only practical access to the very small Higgs coupling to light (first generation) fermions, requiring of course the caveat that CP is violated at an observable level in the $H\gamma\gamma$ interaction.

Searching for a non-zero proton EDM in a dedicated storage ring presents an experimental opportunity to improve the current sensitivity by more than three orders of magnitude compared to the current neutron EDM experimental limit.[8] The method we describe is based on the frozen spin method and uses an all-electric lattice, directly measuring the spin precession due to a non-zero EDM in an electric field. The storage ring EDM collaboration has made significant progress in developing the experimental design for an all-electric EDM measurement. In this paper, we describe the fundamental experimental techniques and the specifications of the all-electric storage ring. We also present the systematic errors and the methods developed to address them.

II. EXPERIMENTAL METHOD

The EDM and magnetic moment in terms of the rest frame spin $\mathbf{s}$ are $\mathbf{d} = (\eta e/2mc)\mathbf{s}$ and $\boldsymbol{\mu} = (ge/2m)\mathbf{s}$, respectively, where these relations define g and η, $G = (g-2)/2$ defined, and m is the particle mass. At rest, the spin precession of a particle in electric and magnetic fields $\mathbf{E}$ and $\mathbf{B}$ is governed by

$$\frac{d\mathbf{s}}{dt} = \boldsymbol{\mu}\times\mathbf{B} + \mathbf{d}\times\mathbf{E}. \tag{1}$$

For a particle with velocity $\boldsymbol{\beta} = \mathbf{v}/c$, relativistic factor $\gamma = \left(1 - v^2/c^2\right)^{-1/2}$, $\boldsymbol{\beta}\cdot\mathbf{E} = 0$, and $\boldsymbol{\beta}\cdot\mathbf{B} = 0$, the spin precesses relative to the momentum with angular velocity $\boldsymbol{\omega}_a + \boldsymbol{\omega}_e$,[9–11] where

$$\begin{aligned}\boldsymbol{\omega}_a &= \frac{e}{m}\left[G\mathbf{B} - \left(G - \frac{1}{\gamma^2-1}\right)\frac{\boldsymbol{\beta}\times\mathbf{E}}{c}\right],\\ \boldsymbol{\omega}_e &= \frac{\eta e}{2m}\left(\frac{\mathbf{E}}{c} + \boldsymbol{\beta}\times\mathbf{B}\right).\end{aligned} \tag{2}$$

Spin precession in a storage ring has been successfully used to establish a limit on a muon EDM.[12,13] For certain $\mathbf{E}$ and $\mathbf{B}$ fields, the $(g-2)$ precession of the particle $\boldsymbol{\omega}_a$ vanishes.[14–17] Thus, aside from an EDM contribution, the spin is frozen along the momentum direction. With $\mathbf{B} = 0$ and the "magic" $\gamma = \sqrt{1 + 1/G}$ chosen, $\boldsymbol{\omega}_a = 0$ and $\boldsymbol{\omega}_e = (\eta e/2mc)\mathbf{E}$. The parameters for this condition in the case of a proton are shown in Table I. In an all-electric storage ring,[18,19] a radial electric field causes the spin to precess out of the storage plane linearly on the time scale of the fill. Details of a storage ring proton EDM experiment are given in Ref. 20. For long-lived, polarized beams, the gain in sensitivity by using the frozen

TABLE I. "Magic" proton parameters to cancel the $(g-2)$ precession in an all-electric ring.

G_p[21]	γ	β	p	E
1.792 847	1.248 107	0.598 379	0.7007 GeV/c	1.171 GeV

spin method over non-dedicated EDM methods[12,13] is several orders of magnitude.[20]

A. Ring and beam parameters

The all-electric ring geometry will include 40 sections of concentric cylindrical deflectors of 52.3 m bending radius, with 36 straight sections of 2.7 m length and four straight sections of 20.8 m length, adding up to a 500 m circumference. The 2.7 m straight sections will include superconducting quantum interference devices (SQUIDS) as magnetometers and electrostatic alternating gradient quadrupoles, with two polarimeters placed in the longer straight sections. Injection of the beams in opposite directions around the ring will occur in the remaining two 20.8 m straight sections. The deflector electric field will be about 8 MV/m radially inward in the 3 cm spacing between the deflector plates. In principle, it is possible to modify the shape of the deflector plates to include vertical focusing. An electrostatic storage ring of this size would be more than ten times larger than any previous electrostatic ring.[22–24] A simplified storage ring and the detail of the deflector lattice are shown in Figures 1 and 2.

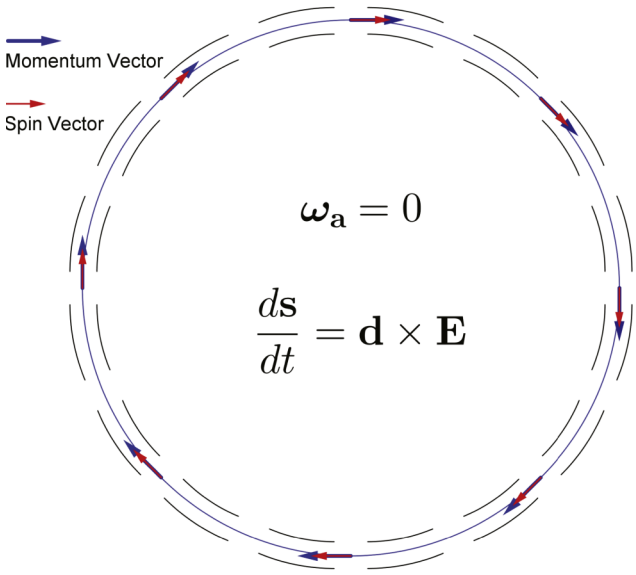

FIG. 1. A conceptual schematic of the storage ring is shown here. The proton beam polarization is kept in the longitudinal direction along the beam momentum, effectively reducing ω_a to zero. The radial electric field acts on the proton EDM (d) for the duration of the storage time and thus significantly increasing the method sensitivity. A realistic lattice will include 40 bending sections separated by 36 straight sections 2.7 m long each, with electrostatic quadrupoles in an alternating gradient configuration, and four 20.8 m long straight sections for polarimetry and beam injection. It will also include SQUID-based magnetometers distributed around the ring, whose total circumference is 500 m.

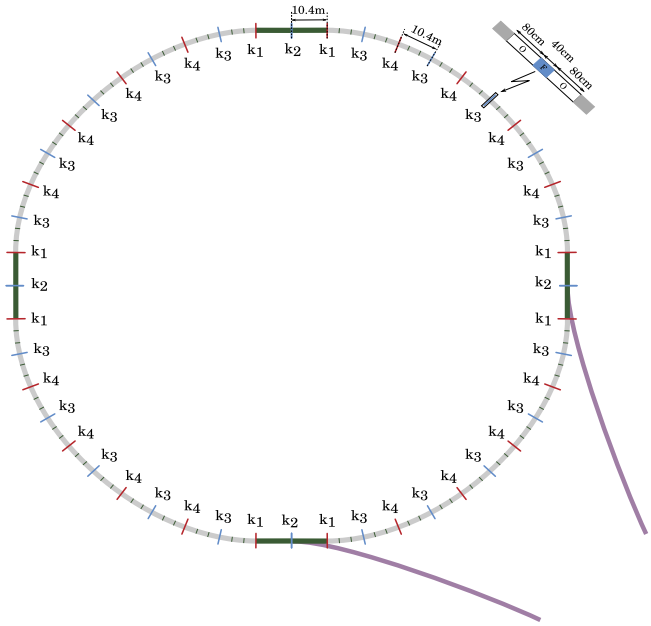

FIG. 2. Details of the storage ring lattice are shown here with focusing and defocusing quadrupoles (shown as k_3 and k_4). The bending sections, including the short straight sections, have a length of 10.417 m, three sections assembled as one unit. The long straight sections are 20.834 m long with a quadrupole (shown as k_2) in the middle and two half-length quads (shown as k_1) at both ends.

B. Experimental techniques

One hundred bunches of 2.5×10^8 vertically polarized protons will be injected in the clockwise (CW) direction and a similar number in the counter-clockwise (CCW) direction, circulating simultaneously. The beams will be allowed to de-bunch and then re-bunch at the required frequency using a high-harmonic ($h = 100$ in this case) RF system. Using an RF solenoid, the spins of the protons will be rotated in the longitudinal direction, producing protons of both positive and negative helicities. The vertical polarization difference between early and late times will determine the average vertical spin precession rate. The considered ring and beam parameters are summarized in Table II.

The horizontal spin coherence time (SCT) of the stored beam is the time required for the RMS spread in spin angles to become one radian. Causes of a finite SCT include horizontal and vertical oscillations as well as longitudinal (energy) oscillations. An RF-cavity is required to keep the SCT much longer than a few ms due to momentum the spread of the beam. The vertical component of the proton spin grows linearly with time, at a rate on the order of nanoradians per second for an EDM detectable by the experiment. In practice, the linear growth of the vertical spin is limited by the SCT of the stored beam. Protons will be stored on the order of 10^3 s, yielding an early-to-late change of the vertical spin component on the order of microradians. A vacuum of better than 10^{-10} Torr is required to keep the beam stored in the ring for 10^3 s.

The electric field of 8 MV/m between the cylindrical deflectors is comparable to previous work which has achieved similar field strengths.[25–27] The effect of the fringe electric fields of the cylindrical deflectors has been investigated both analytically and by precision particle tracking.[28] The bending

TABLE II. Ring and beam parameters of the proton EDM experiment. Proton beam parameters refer to each storage direction.

Bending radius, R_0	52.3 m
Electrode spacing, d	3 cm
Electrode height	20 cm
Deflector shape	cylindrical
Radial E-field, E_0	8 MV/m
Number of straight sections	40
Straight section lengths	2.7389 m, 20.834 m
Polarimeter sections	2
Injection sections	2
SQUID-based magnetometer sections	36
Total circumference, C	500 m
Harmonic number h, RF frequency	100, 35.878 MHz
RF voltage, synchrotron tune Q_s	6 kV, 0.0066
Particles per bunch	2.5×10^8
Maximum momentum spread, $(dp/p)_{\max}$	4.6×10^{-4}
Horizontal beta function, $\beta_{x,\max}$	47 m
Vertical beta function, $\beta_{y,\max}$	216 m
Horizontal dispersion function, $D_{x,\max}$	29.5 m
Horizontal tune, Q_x	2.42
Vertical tune, Q_y	0.44
Vertical emittance, ϵ_{Vmax}	17 mm mrad
Horizontal emittance, ϵ_{Hmax}	3.2 mm mrad
Slip-factor, $\eta=\alpha-1/\gamma^2$	−0.192

radius of the plates has been adjusted to account for additional deflection due to fringe electric fields in the straight sections.

Intrabeam scattering (IBS) effects, increasing the stored beam phase-space parameters, set the time scale of the fill. The storage ring lattice can be optimized to reach equilibrium between the horizontal, vertical, and longitudinal phase-space, making the IBS lifetime large enough not to affect the statistical sensitivity of the method. Such a lattice (below transition) has been achieved resulting in an IBS lifetime of $\gg10^3$ s for a few mA of stored beam current. The resulting space-charge tune shifts are small, with negligible effect on the statistical EDM sensitivity and no known systematic error effects. The beam-beam scattering effects are smaller and do not present a problem.

Polarimeters will be used to measure small changes in the vertical component of the beam polarization by scattering particles from a 6 cm thick carbon target placed in a straight section of the ring lattice so that it is the beam limiting aperture in the vertical direction. The stored beam will be led to collide with the target using a number of possible alternative methods, e.g., by slowly lowering the vertical focusing strength and using a resonant slow extraction vertically. About 99% of the time, the beam particles undergo Coulomb scattering, lose enough energy, and leave the ring. Roughly 1% of the time, the protons undergo spin-dependent nuclear elastic scattering, ending up on a detector located about a meter beyond the target. The scattering of the particles in the up and down (left and right) directions will provide information on the horizontal (vertical) plane polarization component. Detectors must be able to respond to charged-particle events with minimal dead time and small systematic errors. Types under consideration include multi-resistive plate chambers, micro-megas chambers, gas electron multiplier chambers, and silicon

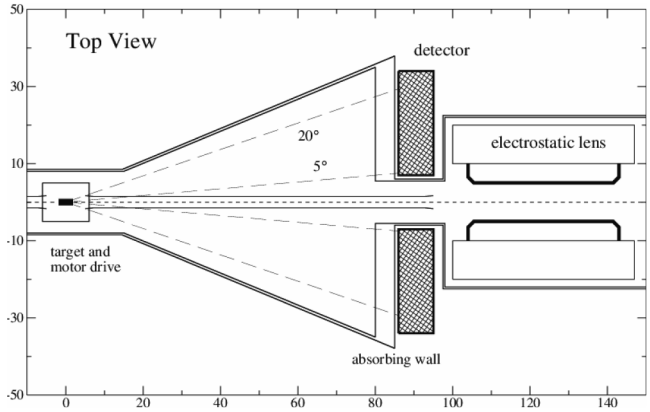

FIG. 3. A top-view of a possible layout of one-half of a proton EDM ring polarimeter, with the horizontal axis along the beam direction and both scales in centimeters. The carbon extraction target is located on a motor drive, placed in a straight section of the ring lattice so that it is the beam limiting aperture in the vertical direction. The beam is denoted by a short-dashed line.

detectors. A polarimeter design under consideration is shown in Figure 3.

A precision tracking program using numerical integration methods such as fourth-order Runge-Kutta and the predictor-corrector method[29] is used to integrate the beam and spin dynamics differential equations. The Runge-Kutta and Predictor-Corrector integration methods used in tracking are slow but accurate; they are kept at a step size on the order of 1-10 ps. The programs have been benchmarked to high accuracy against analytical estimates. Additional programs, such as UAL/ETEAPOT[30,31] or using the Hamiltonian approach,[32] which account for the momentum change of the particle due to motion in E-fields, have been developed. Results from tracking simulations[33,34] confirm that a particle distribution with $(dp/p) = 2\times10^{-4}$ will have an SCT of the order 10^3 s in an idealized lattice. The SCT of the stored beam was found to increase with an increasing ring radius when the lattice design was kept the same.

For a uniform beam extraction rate, the statistical error σ_d of the measurement has been both calculated analytically and confirmed numerically with Monte Carlo simulations to be

$$\sigma_d = \frac{2\hbar}{PAE_0\sqrt{N_{\mathrm{tot,c}}T_{\mathrm{tot}}f\,\tau_{\mathrm{SCT}}}}. \tag{3}$$

Taking parameter values[35,36] of the beam polarization $P = 0.8$, the analyzer power $A = 0.6$, $E_0 = 8$ MV/m over 65% of the ring, $N_{\mathrm{tot,c}} = 5\times10^{10}$ particles per storage cycle (usually referred to as "fill" in accelerators), a particle detection efficiency of $f = 0.011$, a total running time $T_{\mathrm{tot}} = 10^7$ s per year, and a SCT of $\tau_{\mathrm{SCT}} = 10^3$ s, the statistical error for one year is $2.5\times10^{-29}\ e\cdot$cm. The polarimeter analyzing power peaks near the proton "magic" momentum, a fortuitous coincidence. The statistical error, being dependent on the electric field, grows proportionally to the storage ring radius. That error will be reduced by modulating the data-taking rate, taking most of the data at early and late times. In addition, by further optimizing the ring lattice, reducing IBS and increasing SCT, we expect to be able to achieve a statistical sensitivity of $<2\times10^{-29}\ e\cdot$cm per year.

III. SYSTEMATIC ERRORS

Analytical estimates in combination with precision tracking allow the size of potential systematic errors to be estimated in several ways. Magnetic shielding, beam position monitors (SQUID-based Beam position monitors (BPMs) sensitive to B-fields, plus button-BPMs sensitive to E-fields), and lattice alignment to better than 0.1 mm around the ring are sufficient to address the main systematic errors, i.e., radial B-fields[20] and geometric phases.[37,43]

A. Radial B-fields

The ring will be shielded from the Earth's magnetic field as well as from noise through passive shielding and feedback mechanisms. The presence of a net radial B-field, $\langle B_r \rangle$, could mimic an EDM signal, producing a vertical spin precession

$$\omega_V = \frac{eg\langle B_r \rangle}{2m\gamma^2}. \tag{4}$$

An average radial field of 10 aT will cause a spin precession at the sensitivity of the EDM experiment. However, the radial magnetic field would split the CW and CCW beams vertically. The vertical beam position δy as a function of the modes of the radial B-field is

$$\delta y = \sum_{N=0}^{\infty} \frac{\beta c R_0 B_{r,N}}{E_0(Q_y^2 - N^2)} \cos(N\theta + \varphi_N), \tag{5}$$

where Q_y is the vertical tune, which will oscillate between 0.44 and 0.48 at a frequency on the order of 10 kHz.

As noted above, the counter-rotating beams will be split vertically, with maximum separation equal to twice that given by Equation (5). For a 10 aT magnetic field, the split between the beams is on the order of a picometer. Beam position monitors (BPMs) are required that can determine the vertical positions of the CW and CCW beams with picometer-scale resolution over the 10^7 s duration of the experiment. SQUID magnetometers are suitable to measure the magnetic field resulting from the splitting of the CW and CCW beams. Low-temperature DC SQUIDs have demonstrated sensitivities down to 1 fT/$\sqrt{\text{Hz}}$.[38,39] Measuring an average splitting between the CW and CCW beams on the picometer level is feasible with appropriate SQUID placement in the straight sections of the lattice. In principle, no magnetic shielding will be required with continuous BPM measurement around the ring. The finite number of detectors limits the magnetic field modes to which the system is sensitive by the Nyquist sampling theorem. The critical parameter is the detected average radial B-field and that can be wrong only when the mode is equal to the number of the BPM locations around the ring as well as its integer multiples. However, it has been shown analytically as well as by beam/spin tracking simulations that the SQUID-based BPMs are quite insensitive to higher harmonics of the radial B-fields. SQUIDS are sensitive to time dependent B-fields only. The ratio of the time oscillating component of $N = 0$ to higher harmonics can be shown to be $(Q_y/N)^4$, making the high N harmonic contributions negligible. The shielding requirements are dominated by the so-called geometric phase effect (see below). For this reason, the total magnetic field will be shielded to below 10-100 nT at all points in the ring. Such a shielding of the B-field is within the present state of the art.[40]

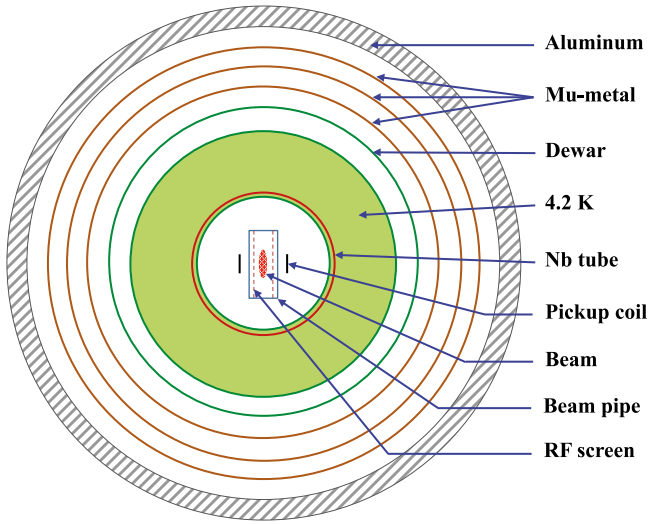

FIG. 4. A schematic of a possible SQUID BPM station, not to scale. The system is shielded with a superconducting Nb tube, Al tube for RF-shield, and several mu-metal layers. The beam-pipe dimensions are 3×20 cm^2, while the outer diameter of the Al RF-shield is of the order of 1 m.

SQUIDs in the straight-sections of the ring should be sufficient to measure the vertical splitting. A schematic of one such possible SQUID BPM station is shown in Figure 4. The vertical spin precession rate as a function of the detected radial B-field will be plotted, with the EDM signal corresponding to the DC offset in the vertical axis.

B. Geometric phases

In three dimensions, spin rotations about different axes do not commute. This fact contributes to geometric phase-induced false EDMs, a significant systematic error in neutron EDM experiments.[8,37,41] In a storage ring, geometric phases of spin dynamics may be cancelled more simply than in a neutron trap. Consider, for example, the N-modes of two non-commuting perturbations: spin rotation frequency around the vertical axis, $(\delta\omega_V)_N \cos(N\omega_c t)$, and spin rotation frequency around the longitudinal axis, $(\delta\omega_L)_N \cos(N\omega_c t + \phi)$. The presence of these perturbations in the lattice leads[42] to a spin rotation around the radial axis with a frequency $\Omega_R = |(\delta\omega_V)_N(\delta\omega_L)_N \sin\phi/(2N\omega_c)|$, thus imitating an EDM signal. It follows from this formula that in order to cancel the geometric phase $\Omega_R t$, we only need to find, experimentally, a counter-perturbation for either of the two N-modes of the perturbed fields. The same approach can be used for other modes.

Perturbed E- and B-fields induce distortions of the closed orbits, the detection of which will be used to check that the errors are being kept at an acceptable level.[20] With respect to achieving this level, analytical investigation, confirmed by precision beam/spin dynamics simulation,[43] has shown that the geometric effect of B-fields splitting the counter-rotating beams can be kept below the experimental sensitivity if the maximum B-field is kept below the 10-100 nT level

everywhere that E-field errors due to plate misalignments displacing both counter-rotating beams from their ideal location can be addressed by placing BPMs within 0.1 mm of the ideal orbit and that small changes to deflector geometry will adequately compensate for systematic errors due to deflector fringe fields.[28]

C. Polarimetry

An experiment investigating the management of geometric and rate-induced systematic errors in polarimetry was conducted at COSY-Jülich[35,36] with a 1.7 cm carbon block target. Large systematic errors consisting of position and angle changes to the beam were made deliberately in order to generate easily measurable effects. At the level of geometric and rate errors expected for the proton EDM experiment, the results of the COSY-Jülich study indicate how to reduce systematic uncertainties in polarimetry to well below the level of sensitivity. Positive and negative helicity bunches will be stored in the same direction, and a combination of observables will be used to identify systematic errors due to non-linearities.[35,36]

D. Vertical forces

The interaction of the CW and CCW beams may lead to a systematic error: if the two counter-rotating beams do not overlap completely, on average they will feel a vertical force from one another. The problem can be addressed as long as the SQUID BPMs are sensitive to the beam separation size, and feedback can be used to eliminate the signal. Any forces on the beams due to image charges on the top and bottom of the vacuum chamber will be minimized by using vertical metallic plates for almost the entire azimuthal extent of the ring. Results from numerical simulations indicate that the aspect ratio of the quadrupole plates can be chosen to reduce the effect when the counter-rotating beam intensities do not cancel exactly. Sextupole electric fields combined with different CW and CCW beam sizes can create a vertical splitting of the counter-rotating beams, setting the specifications for both. Introducing short runs in between regular-length runs will address systematic errors related to the vertical spin component of the beams being correlated to the protons' phase space parameters. The EDM signal depends on the storage time and generally it is larger the longer the storage time, whereas the systematic error related to sextupole fields depends mainly on the beam phase-space parameters and not on the storage time.

E. Other effects

There are potential systematic errors due to the gravitational field and rotation of the Earth. For example, there is a false-EDM signal due to the vertical E-fields being balanced by the force of gravity at our level of sensitivity. Taking the difference between signals of the CW and CCW beams will cancel this effect. Also, Coriolis and Sagnac[44] effects due to the rotation of the Earth have been found to be below the experimental sensitivity. The RF cavity will account for the slightly different travel times of the CW and CCW beams around the ring by equalizing the frequencies. However, the Sagnac effect may place an upper limit (more than 10^3 s) on how long counter-rotating beams will be stored with longitudinal polarization.

Spin resonances may also contribute to a false EDM signal, although this contribution is decreased in the frozen spin ring by a factor $1/\tau_{SCT}$. In addition, spin and beam resonances coincide in the frozen spin ring, so they will be dealt with together (at a later stage of the project).

A summary of the main systematic errors in the experiment is given in Table III.

TABLE III. Main systematic errors of the experiment and their remediation.

Effect	Remediation
Radial B-field	SQUID BPMs with 1 fT/$\sqrt{\text{Hz}}$ sensitivity eliminate it.
Geometric phase	Plate alignment to better than 100 μm, plus CW and CCW storage. Reducing B-field everywhere to below 10-100 nT. BPM to 100 μm to control the effect.
Non-radial E-field	CW and CCW beams cancel the effect.
Vert. quad misalignment	BPM measurement sensitive to vertical beam oscillation common to CW and CCW beams.
Polarimetry	Using positive and negative helicity protons in both the CW and CCW directions cancels the errors.
Image charges	Using vertical metallic plates except in the quad region. Quad plates' aspect ratio reduces the effect.
RF cavity misalignment	Limiting longitudinal impedance to 10 kΩ to control the effect of a vertical angular misalignment. CW and CCW beams cancel the effect of a vertically misplaced cavity.

IV. CONCLUSIONS

The storage ring EDM collaboration has designed an experiment using the frozen spin method and a dedicated storage ring to measure the proton EDM with an unprecedented sensitivity of $10^{-29}\ e \cdot \text{cm}$. We are currently developing prototypes to optimize the critical systems of the experiment, which include magnetic shielding, SQUID-based BPMs, polarimeter, and electric field plates. In parallel, we are developing software for high precision and high efficiency spin and beam dynamics tracking. The proton EDM measurement will provide a valuable probe of new physics beyond the standard model.

Note added in proof. A recent improvement in the Mercury EDM bound[45] $|d_{\text{Hg}}| < 7.4 \times 10^{-30}\ e \cdot \text{cm}$ can be used to indirectly infer an improved proton EDM bound $|d_p| < 2.0 \times 10^{-25}\ e \cdot \text{cm}$, which is still more than 4 orders of magnitude greater than the projected sensitivity proposed in this paper. That Hg experiment achieved systematic uncertainties below the $10^{-29}\ e \cdot \text{cm}$ goal of our direct proton EDM proposal described in this paper. That provides a

supporting evidence that EDM sensitivities below $10^{-29}\ e \cdot \text{cm}$ are in principle achievable.

ACKNOWLEDGMENTS

We wish to acknowledge support for the polarimetry and spin coherence time measurements at COSY-Jülich by Forschungszentrum Jülich. IBS-Korea (project system code: No. IBS-R017-D1-2015-a00) partially supported this project. DOE partially supported this project under BNL Contract No. DE-SC0012704. Finally, we wish to acknowledge significant contributions from Mr. R. Larsen during the initial high voltage prototype tests at BNL as well as from Dr. B. Khazin (deceased) of Novosibirsk on the deuteron polarimeter concept.

[1]L. Landau, "On the conservation laws for weak interactions," Nucl. Phys. **3**(1), 127–131 (1957).
[2]D. Chang, W. Keung, and A. Pilaftsis, "New two-loop contribution to electric dipole moments in supersymmetric theories," Phys. Rev. Lett. **82**(5), 900 (1999).
[3]C. Q. Geng and J. N. Ng, "CP-violation in η, $K_L \to \mu\bar{\mu}$ decays and electric dipole moments of electron and muon," Phys. Rev. D **42**(5), 1509 (1990).
[4]V. Barger, A. Das, and C. Kao, "Electric dipole moment of the muon in a two Higgs doublet model," Phys. Rev. D **55**(11), 7099 (1997).
[5]W. C. Griffith *et al.*, "Improved limit on the permanent electric dipole moment of Hg 199," Phys. Rev. Lett. **102**(10), 101601 (2009).
[6]J. Engel *et al.*, "Electric dipole moments of nucleons, nuclei, and atoms: The standard model and beyond," Prog. Part. Nucl. Phys. **71**, 21–74 (2013).
[7]A. Czarnecki and W. Marciano, in *Lepton Dipole Moments*, edited by L. Roberts and W. Marciano (World Scientific, Singapore, 2010), ISBN: 978-981-4271-83-7.
[8]C. A. Baker *et al.*, "Improved experimental limit on the electric dipole moment of the neutron," Phys. Rev. Lett. **97**(13), 131801 (2006).
[9]V. Bargmann, L. Michel, and V. L. Telegdi, "Precession of the polarization of particles moving in a homogeneous electromagnetic field," Phys. Rev. Lett. **2**(10), 435 (1959).
[10]T. Fukuyama and A. J. Silenko, "Derivation of generalized Thomas-Bargmann-Michel-Telegdi equation for a particle with electric dipole moment," Int. J. Mod. Phys. A **28**(29), 1350147 (2013).
[11]I. B. Khriplovich, "Feasibility of search for nuclear electric dipole moments at ion storage rings," Phys. Lett. B **444**(1), 98–102 (1998).
[12]G. W. Bennett *et al.*, "Measurement of the negative muon anomalous magnetic moment to 0.7 ppm," Phys. Rev. Lett. **92**(16), 161802 (2004).
[13]G. W. Bennett *et al.*, "Improved limit on the muon electric dipole moment," Phys. Rev. D **80**(5), 052008 (2009).
[14]F. J. M. Farley *et al.*, "New method of measuring electric dipole moments in storage rings," Phys. Rev. Lett. **93**(5), 052001 (2004).
[15]Y. F. Orlov, W. M. Morse, and Y. K. Semertzidis, "Resonance method of electric-dipole-moment measurements in storage rings," Phys. Rev. Lett. **96**(21), 214802 (2006).
[16]Y. K. Semertzidis, "A new experiment for an electric dipole moment of muon at the $10^{-24} e \cdot \text{cm}$ level," in Proceedings of the Workshop on Frontier Tests of Quantum Electrodynamics and Physics of the Vacuum, Sandansky, Bulgaria, 1998.
[17]D. F. Nelson *et al.*, "Search for an electric dipole moment of the electron," Phys. Rev. Lett. **2**(12), 492 (1959).
[18]S. R. Mane, "Orbital dynamics in a storage ring with electrostatic bending," Nucl. Instrum. Methods Phys. Res., Sect. A **596**(3), 288–294 (2008).
[19]S. R. Mane, "Orbital and spin motion in a storage ring with static electric and magnetic fields," Nucl. Instrum. Methods Phys. Res., Sect. A **687**, 40–50 (2012).
[20]V. Anastassopoulos *et al.*, "A proposal to measure the proton electric dipole moment with $10^{-29}\ e \cdot \text{cm}$ sensitivity," by the Storage Ring EDM Collaboration, October 2011, available from http://www.bnl.gov/edm/.
[21]A. Mooser *et al.*, "Direct high-precision measurement of the magnetic moment of the proton," Nature **509**(7502), 596–599 (2014).
[22]S. P. Møller, "ELISA, an electrostatic storage ring for atomic physics," Nucl. Instrum. Methods Phys. Res., Sect. A **394**(3), 281–286 (1997).
[23]T. Tanabe *et al.*, "An electrostatic storage ring for atomic and molecular science," Nucl. Instrum. Methods Phys. Res., Sect. A **482**(3), 595–605 (2002).
[24]R. von Hahn *et al.*, "The electrostatic cryogenic storage ring CSR - Mechanical concept and realization," Nucl. Instrum. Methods Phys. Res., Sect. B **269**(24), 2871–2874 (2011).
[25]S. R. Moore *et al.*, "Improving the Tevatron collision helix," in Particle Accelerator Conference, 2005, PAC 2005. Proceedings of the IEEE, 2005.
[26]M. BastaniNejad *et al.*, "Improving the performance of stainless-steel DC high voltage photoelectron gun cathode electrodes via gas conditioning with helium or krypton," Nucl. Instrum. Methods Phys. Res., Sect. A **762**, 135–141 (2014).
[27]M. BastaniNejad *et al.*, "Evaluation of niobium as candidate electrode material for dc high voltage photoelectron guns," Phys. Rev. Spec. Top.: Accel. Beams **15**(8), 083502 (2012).
[28]E. Metodiev *et al.*, "Fringe E-fields of flat and cylindrical deflectors in electrostatic charged particle storage rings," Phys. Rev. Spec. Top.: Accel. Beams **17**(7), 074002 (2014).
[29]R. W. Hamming, "Stable predictor-corrector method for ordinary differential equations," J. ACM **6**, 37–47 (1959).
[30]N. Malitsky and R. Talman, "Status of unified accelerator libraries (UAL)," in *Proceedings of the Particle Accelerator Conference, 1997* (IEEE, 1997), Vol. 2.
[31]L. Schachinger and R. Talman, "TEAPOT, thin element tracking program for optics and tracking," Part. Accel. **22**, 35 (1987), available at https://lib-extopc.kek.jp/preprints/PDF/1986/8602/8602067.pdf.
[32]S. R. Mane, "Synchrobetatron coupling in a storage ring with transverse electrostatic fields," Nucl. Instrum. Methods Phys. Res., Sect. A **758**, 77–82 (2014).
[33]S. Hacıömeroğlu and Y. K. Semertzidis, "Results of precision particle simulations in an all-electric ring lattice using fourth-order Runge-Kutta integration," Nucl. Instrum. Methods Phys. Res., Sect. A **743**, 96–102 (2014).
[34]S. R. Mane, "Comment on 'Results of precision particle simulations in an all-electric ring lattice using fourth-order Runge-Kutta integration,"' Nucl. Instrum. Methods Phys. Res., Sect. A **769**, 26–31 (2015).
[35]A. Imig and E. Stephenson, "Measurement of systematic error effects for a sensitive storage ring EDM polarimeter," APS Meeting Abstracts, Vol. 1, 2009.
[36]N. P. M. Brantjes *et al.*, "Correcting systematic errors in high-sensitivity deuteron polarization measurements," Nucl. Instrum. Methods Phys. Res., Sect. A **664**(1), 49–64 (2012).
[37]M. V. Berry, "Classical adiabatic angles and quantal adiabatic phase," J. Phys. A: Math. Gen. **18**(1), 15 (1985).
[38]Y. H. Lee *et al.*, "Double relaxation oscillation SQUID systems for biomagnetic multichannel measurements," IEICE Trans. Electron. **88**(2), 168–174 (2005).
[39]W. Vodel and K. Makiniemi, "An ultra low noise DC SQUID system for biomagnetic research," Meas. Sci. Technol. **3**(12), 1155 (1992).
[40]See http://www.ptb.de/cms/fileadmin/internet/fachabteilungen/abteilung_8/8.2_biosignale/8.21/mssr.pdf for Berlin magnetically shielded room.
[41]J. M. Pendlebury *et al.*, "Geometric-phase-induced false electric dipole moment signals for particles in traps," Phys. Rev. A **70**(3), 032102 (2004).
[42]Y. F. Orlov, "In the EDM experiment, the radial electric field must compensate the vertical magnetic field locally, not on the average," Storage-Ring EDM Collaboration EDM Note #26, December 2002.
[43]S. Haciomeroglu *et al.*, "Geometric effect in the all electric storage ring proton EDM experiment" (unpublished).
[44]G. Sagnac, "L'éther lumineux démontré par l'effet du vent relatif d'éther dans un interféromètre en rotation uniforme," C. R. Acad. Sci. **157**, 708–710 (1913).
[45]B. Graner *et al.*, "Reduced limit on the permanent electric dipole moment of ^{199}Hg," Phys. Rev. Lett. **116**, 161601 (2016).